Dynamics of Rigid Rotors in Retainer Bearings

M. FUMAGALLI, B. FEENY AND G. SCHWEITZER

ABSTRACT

We present results on the dynamics and loads of a rigid rotor in a simple rigid bearing with clearance. For a sliding rotor in "cylindrical motion" with Coulomb friction, the nonlinear solution yields information on the effects of both the coefficient of friction and the air gap on such motion. A more general model indicates when cylindrical and "conical" motions exist. At high speeds, cylindrical motions produce the highest bearing loads, although loads are also intolerable for conical motions.

INTRODUCTION

The major obstacle facing the active-magnetic-bearing (AMB) industry lies in the "retainer bearings." The purpose of these bearings (also referred to as auxiliary, backup, touchdown, and safety bearings) is to retain the rotor from the magnetic bearing assembly and circuitry in the event of AMB failure. Most current designs extend little beyond the mere presence of these auxiliary bearings, along with prayers for their successful function. Practical concerns regard the ability to protect the AMB assembly, and the lifetime of retainer bearings. A thorough understanding of the dynamics of rotors in retainer bearings is imperative if the magnetic-bearing technology is to reach its full potential.

We mention examples of existing studies relevant to this problem. Black [1] examined resonance vibrations in an elastic rotor limited by an annular clearance. Kim and Noah [2] have performed nonlinear analyses on synchronous motions of elastic rotors with bearing clearances. Ishii and Kirk [3] numerically simulated rotor drop in a system that modeled the dynamics of the rotor, bearing contacts, inner race, bearing, and housing. Experiments have been performed by Dell *et al.* [4] on large retainer bearings.

This study examines rigid, balanced rotors in various motions. There is a general understanding that a rotor can undergo cylindrical or conical motions (Figure 1). It is of interest to know if these modes exist and are stable, and if they can be used, at least as limiting cases, for determining loads on the bearings. The goal is to understand the dynamics of these models under frictional excitations, and to briefly examine the implications of general motions and gyroscopic effects on bearing loads.

Institute of Robotics, ETH Zürich, CH-8092 Zürich, Switzerland

ASSUMPTIONS AND MODELING

The assumptions in all of the models are as follows. The rotor and bearing housing are considered to be rigid and perfectly balanced. Rigidity simplifies the analysis and yields dynamics due to friction and, when applicable, gyroscopic forces. Frictional sliding is modeled with the Coulomb friction law. For most of this work, we assume that the rotor is horizontal and the relative rotation speed is much larger than the revolution speed, so that during contact the bodies are always sliding. This corresponds to a rotor with an enormous initial rotation rate. We also assume that the impact phase has settled out, and permanent contact takes place thereafter. We are aware that the transition to permanent contact is characterized by highly nonlinear dynamics with potentially chaotic motion [5]. No applied torques are included.

Considering a rigid rotor in a rigid bearing, general sliding motion can be thought of as consisting of two "modes": cylindrical and conical (Figure 1). The actual sliding dynamics can be described as a combination of these modes.

The *cylindrical model* is built on the assumption that cylindrical motion exists and is stable. Figure 2 shows coordinates describing circumferential motion and rotor rotation. In order to examine the existence and stability of cylindrical motion, the *general model* is developed by adding a degree of freedom in order to characterize motion in the neighborhood of the purely cylindrical mode (Figure 3).

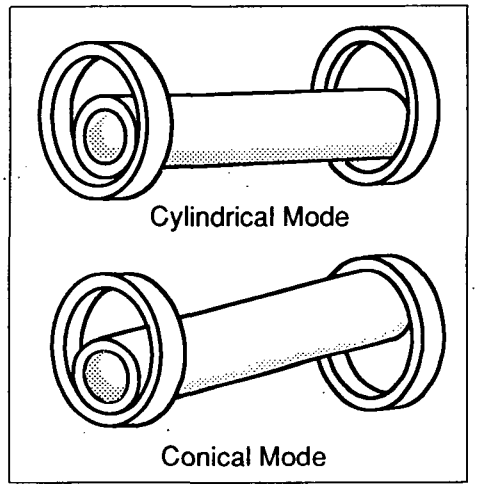

Figure 1. Hypothetical Motions

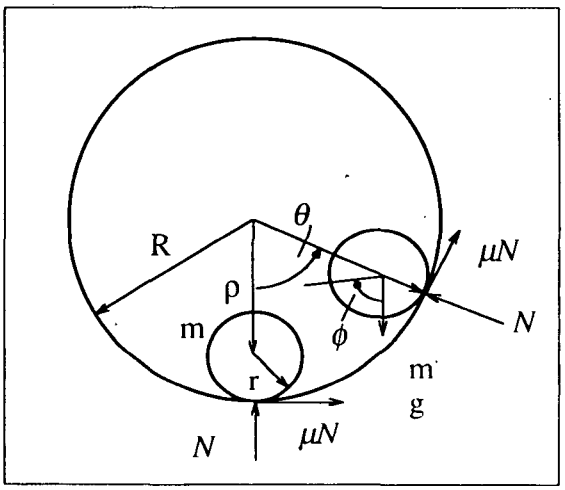

Figure 2. Cylindrical Motion

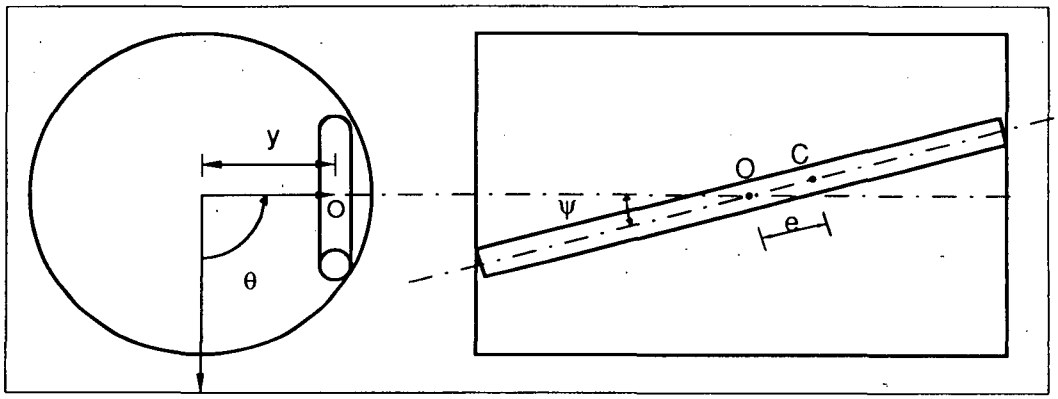

Figure 3. General Model

CYLINDRICAL MODEL

The free-body diagram or a rotor undergoing stable, cylindrical gliding is shown in Figure 2. The circumferential coordinate is θ (also referred to as revolution) and the spin is represented by ϕ and its time derivative $\dot{\phi}$. The rotor has mass m, rotational inertia J, and radius r. The bearing has radius R. The air gap, which is the radius from the center of the bearing to the center of mass, is ρ. The parameter μ represents the coefficient of sliding friction, and g represents gravitational acceleration.

The equations of motion for the model of Figure 2 can be derived by summing the forces on the rotor. The friction force $f(v_r)$, where v_r is the relative sliding velocity, is modeled with the Coulomb law. In our application, $v_r = \rho\dot{\theta} - r\dot{\phi}$. When $r\dot{\phi} > \rho\dot{\theta}$, indicating relative sliding, we have $f(\rho\dot{\theta} - r\dot{\phi}) = \mu$ and

$$m\rho\ddot{\theta} + mg\sin\theta - \mu m(g\cos\theta + \rho\dot{\theta}^2) = 0. \tag{1}$$

The equation for the rotor speed, $\dot{\phi}$, if needed, is

$$J\ddot{\phi} + \mu mr(g\cos\theta + \rho\dot{\theta}^2) = 0. \tag{2}$$

Equations (1) and (2) are valid for nonnegative normal loads, i.e. $g\cos\theta + \rho\dot{\theta}^2 \geq 0$.

ANALYTICAL SLIDING SOLUTION

If there is relative sliding, $\dot{\phi}$ has no effect on equation (1) other than to produce a constant friction term μ. If $\dot{\phi}$ is large, relative sliding should occur for some time. Under this assumption, we neglect the rotor speed $\dot{\phi}$ and analyze the dynamics of equation (1) for all initial conditions in θ and $\dot{\theta}$, provided contact is maintained.

Equation (1) is solvable. Nondimensionalizing (1) and introducing a change of coordinates $\xi = \theta + \beta - \pi/2$ put the equations, expressed as a first-order system, in a form convenient for the analysis of revolution:

$$\dot{\xi} = \eta, \qquad \dot{\eta} = -\alpha\sin\xi + \mu\eta^2. \tag{3}$$

where $\alpha = (g/\rho)\sqrt{1+\mu^2}$ and $\beta = \tan^{-1}(1/\mu)$. The origin of our original system lies at $\xi = \beta - \pi/2$ in the new coordinate system. The region of validity, based on a positive normal load, becomes $g\sin(\xi+\beta) + \rho\dot{\xi}^2 \geq 0$. The fixed points are $(0,0)$, which is a center, and $(\pm\pi, 0)$, which is a saddle. If we look at $\dot{\eta}/\dot{\xi}, \eta \neq 0$, we can solve for η^2:

$$\eta^2 = \frac{2\alpha}{1+4\mu^2}(2\mu\sin\xi + \cos\xi) + Ce^{2\mu\xi}, \tag{4}$$

where C is a constant of integration. The numerically integrated phase trajectories in the original coordinate system are plotted in Figures 4 and 5.

The phase trajectories include a homoclinic orbit, which is the loop coming from the saddle and encompassing the center. Inside the homoclinic orbit are periodic, oscillatory motions. Outside the homoclinic orbit are circular motions, during which the rotor circumnavigates the bearing. Friction opposes the clockwise circulatory motions,

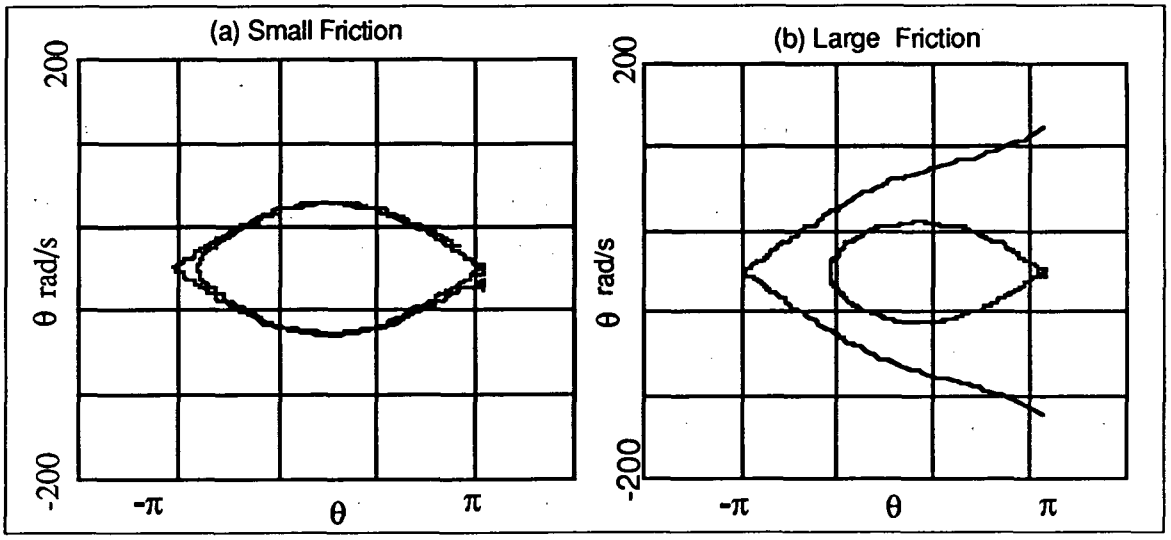

Figure 4. Phase portrait for (a) small friction (b) large friction

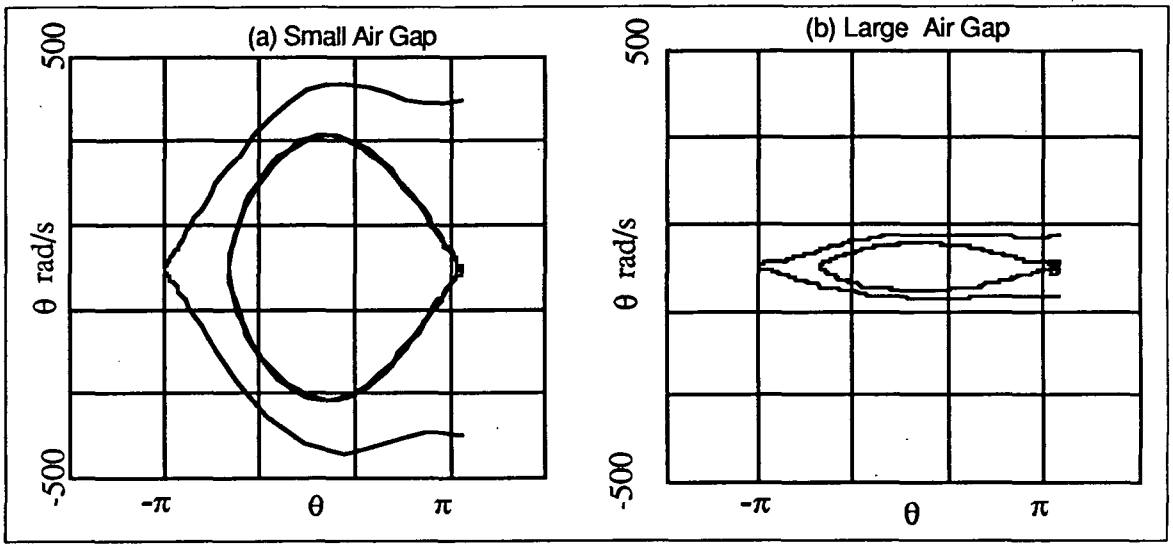

Figure 5. Phase portrait for (a) small air gap (b) large air gap

which slow down, reverse direction (between the homoclinic loop and the saddle) and increase speed counterclockwise. Meanwhile, $\dot{\phi}$ decreases due to frictional damping. In this way $\dot{\theta}$ increases and $\dot{\phi}$ decreases until $\rho\dot{\theta} = r\dot{\phi}$, when rolling starts.

When orbits cross into the region in which the normal load is negative, contact is lost and the equations are no longer valid. Freefall and impacts would follow.

EFFECTS OF PARAMETERS

For pure sliding, as long as the parameters μ, ρ, and g are positive for physical considerations, there are no bifurcations in the sliding system, meaning there are no qualitative changes in the phase trajectories. The effect of the parameters is to deform the phase trajectories, and therefore to influence the "likelyhood" of each type of deterministic behavior. "Likelyhood" refers to a randomly chosen initial condition.

Considering friction, we note that α depends on μ. Motion for small μ, shown in Figure 4a, approaches pendulum behavior. As $\mu \to \infty$ (which may be unrealistic), the homoclinic orbit is squashed toward the origin (Figure 4b). The location of the origin of the original coordinate system goes from zero for $\mu = 0$ to $\pi/2$ for large μ. Combining these effects, increasing μ will increase the likelyhood of circular motion.

For small ρ, the homoclinic is stretched in the $\dot{\theta}$ (η) direction (see Figure 5a). also gets As ρ increases, the phase portrait is squashed in the $\dot{\theta}$ direction (Figure 5b). However, this feature may lead us to the wrong conclusions. In fact, as ρ decreases, the likelyhood of circular motions increases.

In effort to explain this, we consider that an arbitrary initial condition arises from disturbances of certain energy levels. The kinetic energy of revolution is proportional to the square of velocity v. Since $\dot{\theta} = v/\rho$, not only does the phase portrait stretch with decreasing ρ, but the $\dot{\theta}$ axis stretches as well. It turns out that the $\dot{\theta}$ axis stretches faster than the phase portrait. Hence, the homoclinic loop *stretches* in velocity v as ρ *increases*. When thinking in terms of rectilinear velocities as initial conditions, a small ρ leads to a high probability these initial conditions lie in regions of circular motions.

Intuitively, one expects the capability of circular motions to increase with decreasing ρ. Increasing ρ increases the potential difference between the top and the bottom of the bearing. Furthermore, given an initial velocity v, the centripetal normal load is inversely proportional to ρ, producing higher frictional excitation with smaller ρ.

The rotor radius r does not appear in the θ equation for sliding. Thus, the *sliding* dynamics of θ have no dependence on r. However, r effects the sliding dynamics of ϕ. For large r, there is a great frictional torque on ϕ. Also the rolling condition, $r\dot{\phi} = \rho\dot{\theta}$, is effected. Hence, $\dot{\phi}$ slows down rapidly, and rolling takes place more quickly.

NUMERICAL SIMULATION

The above analysis assumes relative sliding. A numerical simulation of equations (1) and (2) can provide some indication of how long this assumption may be reasonable. In the simulation, $m = 7.76$ kg, $J = 2.425$ g/m/m, and $\rho = 0.3$ mm.

This simulation yields information about the effects of initial values of $\dot{\phi}$ for the specific case of initial conditions $\theta = \dot{\theta} = 0$ (bottom of the bearing). In Figure 6, parameter values in one region lead to either oscillations or impacting motions. Parameter values in the other region lead to circular revolutions. Two factors may eliminate the possibility of circular motions for this initial condition: low friction, or low duration of frictional excitation. The analysis of sliding motion shows that as the friction increases, the potential for circular revolutions increases. However, as one might expect, if the initial rotation rate $\dot{\phi}$ is too small, rolling will commence prior to achieving circular revolutions, and the rotor will drop or oscillate.

HIGH-VELOCITY APPROXIMATION

If $\dot{\theta}^2 \gg g/\rho$, letting $\Omega = \dot{\theta}$, and $\omega = \dot{\phi}$, and stretching time such that $\tau = \mu t$, equations (1) and (2) can be approximated as $\Omega'(\tau) = \Omega^2(\tau)$ and $\omega'(\tau) = -mr\rho\Omega^2(\tau)/J$.

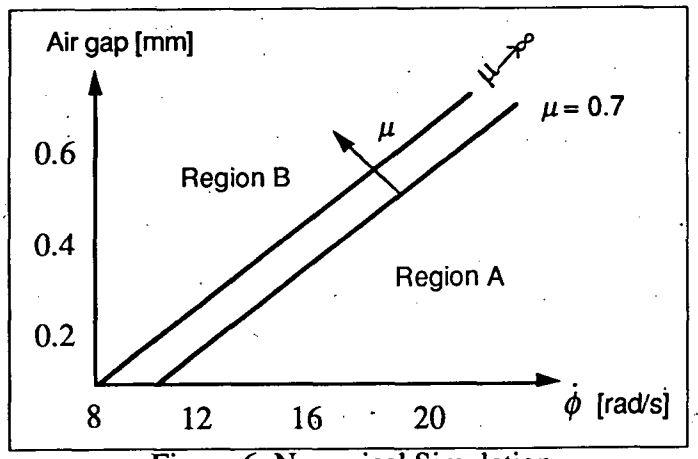

Figure 6. Numerical Simulation

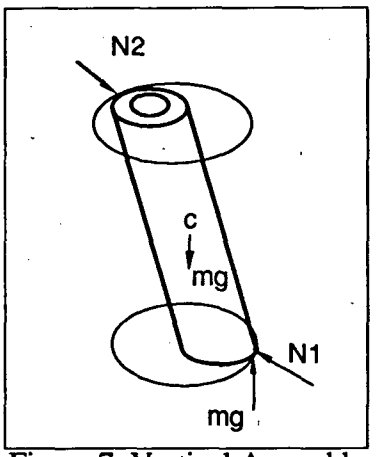

Figure 7. Vertical Assembly

The solution to these equations is

$$\Omega = \frac{\Omega_0}{1 - \Omega_0 \tau}, \qquad \omega = \omega_0 - \frac{mr\rho}{J} \frac{\Omega_0^2 \tau}{(1 - \Omega_0 \tau)}, \tag{5}$$

valid until rolling begins, where Ω_0 and ω_0 are the "initial" conditions at $\tau = 0$.

There are two important results in this approximation. First, if we disregard the rolling condition, the solution shows $\Omega \to \infty$ in *finite time*. Of course, rolling will occur first, but there may be an enormous increase in Ω. Second, the friction μ effects only the time scale, and not the magnitudes or shapes of solutions. This means that, in the high-velocity approximation, the velocities achieved at rolling are *independent* of μ. Important to rolling is the ratio $mr\rho/J$. Maximizing this ratio minimizes the rolling velocities of ω $(=\dot{\phi})$, and hence Ω $(=\dot{\theta})$.

GENERAL MODEL

We use two different models: one for nearly cylindrical motions, and the other for nearly conical motions. The coordinate systems are sketched in Figure 3. The rod has length $2L$, radius r, rotational inertias J and I, and longitudinal imbalance e marking the distance between the geometric center of the rotor and its center of mass.

To describe nearly cylindrical motion, we look at the revolution $\theta(t)$ of the center of the rotor, and the rotor's angular deviation $\psi(t)$ from purely cylindrical motion. The angular position $\psi(t)$ and the ratio ρ/L are assumed to be very small. For nearly conical motion, we look at the revolution $\theta(t)$ of the center of the rotor, and its radial displacement $y(t)$ from the center of the bearing housing. The constraint of contact with the bearings, $\psi = \sqrt{\rho^2 - y^2}/L$, affects the development of the equations of motion.

The nearly cylindrical description is singular at $\psi = \rho/L$, and, in turn, the nearly conical description is singular at $y = \rho$. This singularity arises from the derivative of constraint relationship between ψ and y. As a result, neither description can be used to analyze the global behavior. Therefore motions neighboring purely cylindrical and purely conical motions are studied. Hence, the equations are linearized in ψ and in y.

The system was assumed to have no translation in the axial direction. We used Lagranges equations of motion for the system with the above coordinates:

$$\frac{d}{dt}\frac{\partial T}{\partial \dot{r}_i} - \frac{\partial T}{\partial r_i} - F_i = Q_i, \tag{6}$$

where r_i are generalized coordinates. We calculated the normal loads at the contact points by summing forces and moments about the center of gravity of the rotor. Multiplying the normal loads by the coefficient of friction μ produced generalized forces Q_i. The other forces and moments F_i are conservative.

The equations of motion were derived for the horizontal geometry and the vertical geometry (see Figure 7) of an untorqued system. Lengths are normalized to an air gap of one. The resulting equations are long, and hence not shown. We look for cylindrical and conical solutions. For simplicity, we analyze the special case of $e = 0$. Although this does not usually occur in the real systems which motivate this work, it could occur by design if the retainer bearings were placed appropriately.

First we consider the horizontal geometry. When $e = 0$, the equation representing a sum of moments in the ψ direction in the nearly cylindrical description reduces to

$$I\ddot{\psi} + J\dot{\theta}\dot{\phi}\psi - (I-J)\dot{\theta}^2\psi + mL^2\dot{\theta}^2\psi + mgL^2\psi\cos\theta = \mu(I\ddot{\theta}\psi + (2I-J)\dot{\theta}\dot{\psi} - J\dot{\phi}\dot{\psi}), \tag{7}$$

which admits $\psi(t) \equiv 0$ is a solution. Hence, cylindrical motion is a solution for the horizontal geometry. For small oscillations in θ this motion has regions of stability and instability in parameter space [6]. (However, when $e \neq 0$, $\psi(t) \equiv 0$ is *not* a solution.)

In the nearly conical description with $e = 0$, the equation representing a sum of forces in the y direction reduces to

$$m\ddot{y} - my\dot{\theta}^2 - \frac{J}{L^2}y\dot{\theta}\dot{\phi} - \frac{(J-I)}{L^2}y\dot{\theta}^2 - mg\cos\theta = -\mu m(y\ddot{\theta} + 2\dot{y}\dot{\theta}). \tag{8}$$

Because of the $\cos\theta$ term, $y(t) \equiv 0$ with $\theta(t) \neq const$ is *not* a solution! Hence, purely conical motions should not be observed in the rotors. (This is also true for $e \neq 0$.) Physically, this makes sense. If a rotor were to have $y = 0$ as it passed through $\theta = \pi/2$, gravity would force it away from $y = 0$. If the rotor were in a zero-gravity environment, however, the $\cos\theta$ term drops out and the conical solution would exist.

The equations for the vertical geometry assume a set-up similar to the milling spindels of Mecos AG [7]. In this arrangement (Figure 7), the support (which prevents the rotor from falling out of the assembly) is applied to the outer edge of the rotor by the lower bearing. For $e = 0$, the equations for nearly pure cylindrical motions are

$$I\ddot{\psi} + J\dot{\theta}\dot{\phi}\psi - (I-J)\dot{\theta}^2\psi + mL^2\dot{\theta}^2\psi = \mu(I\ddot{\theta}\psi + (2I-J)\dot{\theta}\dot{\psi} - J\dot{\phi}\dot{\psi} - mgr + (L+rL)mg\psi).$$

This time, $\psi(t) \equiv 0$ is *not* a solution. Physically, this is because the frictional load at the support end of the rotor is larger than that of the other end, since friction comes from radial (centripetal) loads and from the axial gravitational support load. Thus, the frictional loading is not in equilibrium during hypothetical cylindrical motion.

Finally, for nearly conical motion in the vertical geometry, $e = 0$,

$$m\ddot{y} - my\dot{\theta}^2 - \frac{J}{L^2}y\dot{\theta}\dot{\phi} + \frac{I}{L^2}y\dot{\theta}^2 = -\mu m(y\ddot{\theta} + 2\dot{y}\dot{\theta} + g(1 + \frac{1}{L})). \tag{10}$$

Again, $y(t) \equiv 0$ is not a solution (unless the rotor operates in zero gravity). Thus, purely conical motion should not be observed. The physical interpretation is similar to that of the vertical cylindrical case.

In the vertical geometry, because the support end of the rotor undergoes higher frictional loading than the "free" end, one might expect the support end to circumnavigate its bearing faster than the free end. Since the motion is likely to be extremely fast, it may be difficult for the casual observer to distinguish it from, say, conical motion. To analyze such general motion would require globally valid equations.

LOADS DURING MOTIONS

The normal loads were calculated while determining the equations of motion. Here we discuss the loads for cylindrical and conical motions. Indeed, it is possible that the rotor will not be seen near cylindrical or conical motion. Instead, the dynamics may dance around one mode or the other, or even between them. Certainly the motion will at times be nearby cylindrical motion, or nearby conical motion. At such instances, the normal load estimates are valid.

The general expressions for the normal loads in each bearing during nearly cylindrical and nearyl conical motions are

$$N_{cyl} = \frac{m(L \pm e)}{2L}(\rho\dot{\theta}^2 + g\cos\theta + e\ddot{\theta}\psi + 2e\dot{\theta}\dot{\psi}) \pm \frac{1}{2L}(I\ddot{\psi} + (2I - J)\dot{\theta}\dot{\psi} - J\dot{\psi}\dot{\phi}), \tag{11}$$

$$N_{con} = \frac{m(\pm(L^2 + r\rho) - eL)}{2(L^2 + \rho r)}(y\ddot{\theta} + 2\dot{y}\dot{\theta} - \frac{e\rho}{L}\dot{\theta}^2) + \frac{(I - J)\dot{\theta}^2\rho - J\rho\dot{\theta}\dot{\phi}}{2(L^2 + \rho r)}. \tag{12}$$

The air gap is typically small in industrial applications. In such case, we can formulate a worst-case scenario for $e = 0$. In purely cylindrical motions, $\dot{\theta}$ increases while $\dot{\phi}$ decreases until the onset of rolling, at which time $\dot{\phi} \approx \dot{\phi}_{roll}$. If we employ the kinematic relationship of rolling, $r\dot{\phi} = \rho\dot{\theta}$, then the dominating term describing the normal loads for each bearing during cylindrical circular motion is given by

$$N_{cyl} = \frac{mr^2\dot{\phi}_{roll}^2}{2\rho}. \tag{13}$$

As the air gap gets small, and as the velocity gets high, both typical for magnetic-bearing applications, the normal load becomes extremely high. (In the limiting case as $\rho \to 0$, rolling is not possible since $\dot{\phi} = \rho\dot{\theta}/r$ and infinite $\dot{\theta}$ loses meaning.)

As an example, we numerically integrated equations (1) and (2) numerically for a balanced rotor with $\mu = 0.01$, $m = 7.76$ kg, $r = 25$ mm, $\rho = 0.3$ mm. The initial conditions where $\theta = 0, \dot{\theta} = 600$ rad/s (corresponding to an initial rectilinear velocity of about 20 cm/s), and $\dot{\phi} = 1000$ rad/s. The histories of $\dot{\phi}, \dot{\theta}$, N_{cyl}, and dissipation power P are shown in Figure 8. Rolling first took place after 0.18 seconds with a

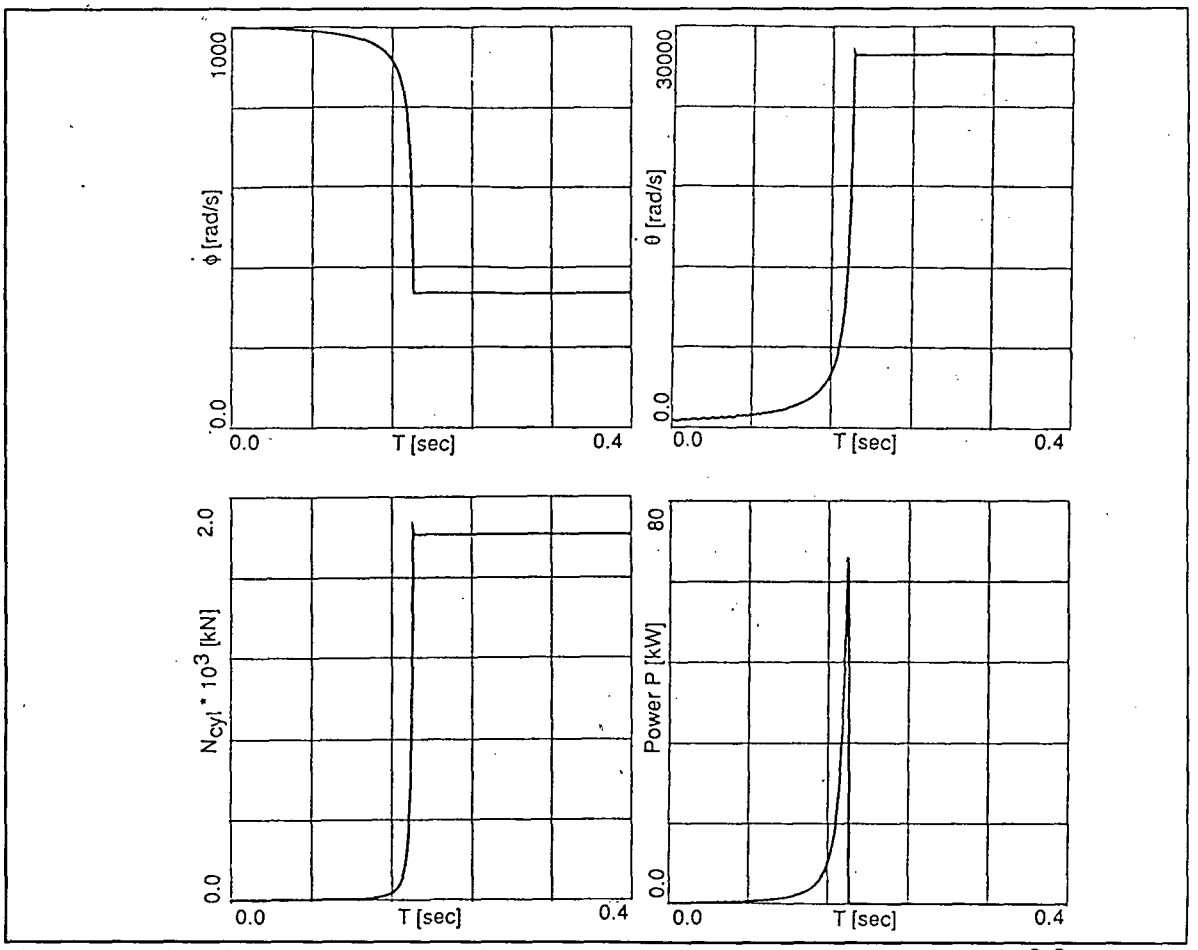

Figure 8. Velocities, Force, Power with m = 7.76 Kg, r = 25 cm, μ = 0.01, ρ = 0.3 mm. The initial conditions are $\dot{\phi}$ = 1000 rad/s, $\dot{\theta}$ = 600 rad/s.

value of $\dot{\phi} = 320$ rad/s, at which time the normal load was maximum at $N_{cyl} = 1800$ kN. Such a normal load cannot be withstood. Certainly the model will have broken down prior to reaching such a load. This breakdown in the model may correspond to the destruction of the bearing. The plots feature initially gradual changes in these quantities, followed abruptly by enormous changes. (Recall that, in the mathematics of sliding at high velocities, $\dot{\theta} \to \infty$ in finite time). While $\dot{\theta}$ increases rapidly, so does N_{cyl}, which in turn causes $\dot{\phi}$ to decrease rapidly until rolling commences. For values of $\mu = 0.1$ and $\mu = 0.001$ the pictures are nearly the same except for a profound change in the time scale. This time scale property affects the power dissipation, which may have implications for the thermal and wear aspects of this problem. The maximum dissipation power was 70 kW. The power of dissipation is directly proportional to μ ($P_{max} = 700$ kW for $\mu = 0.1$). Such a high value for the dissipation power leads to the conclusion that an investigation of the thermal effects will be necessary in the future.

If we examine conical motions in the case of rolling (which may not take place for the conical configuration), the load estimate for each bearing is

$$N_{con} = \frac{(I - J)r^2\dot{\phi}_{roll}^2}{2\rho L^2}. \tag{14}$$

The ratio between the cylindrical load and the conical load is $mL^2/(I-J)$. For a uniform elongated rod with $I/J = 10$, the cylindrical load is approximately three times larger than the conical load during rolling.

Our estimates are for small ρ/L. Other setups may produce additional large terms.

CONCLUDING REMARKS

For cylindrical (synchronous) motions, increasing the friction coefficient and decreasing the air gap increase the likelyhood of circular motions, as opposed to oscillatory motions. This is important because circular motions produce high bearing loads.

In more general models, we have estimated the bearing loads and given examples. Circular cylindrical and conical motions may lead to intolerable bearing loads. When the air gap is small, circular motions are the most dangerous for elongated rotors, producing loads approximately three times as large as in the conical case. The general model also indicates that purely cylindrical motions exist only when the rotor is perfectly balanced in the longitudinal direction. Purely conical motions never exist in gravitational fields.

Based on these results concerning the dynamics and the bearing loads, the initial recommendation is to design retainer bearings with large air gaps and low coefficients of friction, and rotors with a large ratio $mr\rho/J$. Of course other criteria, too, for choosing dimensions and the design of retainer bearings might later be introduced.

ACKNOWLEDGEMENT

The work of M. Fumagalli was funded by CNPQ–Conselho Nacional de Desenvolvimento Científico e Tecnológico, of Brazil.

REFERENCES

[1] Black, H. F., "Interaction of a whirling rotor with a vibrating stator across a clearance annulus," Journal of Mechanical Engineering Science 10(1) 1-12 (1968).

[2] Kim, Y. B, and Noah, S. T., "Bifurcations analysis for a modified Jeffcott rotor with bearing clearances," Nonlinear Dynamics 1, 221-241 (1990).

[3] Ishii, Toshiyasu, and R. Gordon Kirk, "Analysis of rotor drop on auxiliary bearings following AMB failure," ROMAG '91 Magnetic Bearings and Dry Gas Seals Conference, Washington, D. C., March 13-15.

[4] Dell, H., Engel, J., Faber, R., and Glass, D., "Developments and tests on retainer bearings for large active magnetic bearings," First International Symposium on Magnetic Bearings, ETH Zürich 1988, Springer-Verlag 1988.

[5] Szczygielski, W., and Schweitzer, G., "Dynamics of a high-speed rotor touching a boundary," IUTAM/IFTOMM Symposium on Multibody Dynamics, CISM Udine, September 1985, Springer-Verlag, 1986.

[6] Feeny, B., "Stability of cylindrical rotor motion in a retainer bearing," Institut für Robotik, ETH Zürich (1991).

[7] Siegwart, R., "Aktive magnetische Lagerung einer Hochleistungs-Frässpindel mit digitaler Regelung," Dissertation ETH No. 8962, ETH Zürich (1989).